JOURNAL OF Applied Polymer SCIENCE

Investigation on Crystallization Behavior and Hydrophilicity of Poly(vinylidene fluoride)/poly(methyl methacrylate)/Poly(vinyl pyrrolidone) Ternary Blends by Solution Casting

Jing Cheng,[1] Jun Zhang,[1] Xiaolin Wang[2]

[1]College of Materials Science and Engineering, Nanjing University of Technology, Nanjing 210009, People's Republic of China
[2]Department of Chemical Engineering, Tsinghua University, Beijing 100084, People's Republic of China
Correspondence to: J. Zhang (E-mail: zhangjun@njut.edu.cn)

ABSTRACT: Ternary blends composed of matrix polymer poly(vinylidene fluoride) (PVDF) with different proportions of poly(methyl methacrylate) (PMMA)/poly(vinyl pyrrolidone) (PVP) blends were prepared by solution casting. The crystallization behavior and hydrophilicity of ternary blends were characterized by scanning electron microscopy (SEM), Fourier transform infrared spectroscopy (FTIR), wide angle X-ray diffraction (WAXD), differential scanning calorimetry (DSC), and contact angle test. According to morphological analysis, the surface was full of typical spherulitic structure of PVDF and the average diameter was in the order of 3 μm. The samples presented predominantly β phase of PVDF by solution casting. It indicated that the size of surface spherulites and crystalline phase had little change with the PMMA or PVP addition. Moreover, FTIR demonstrated special interactions among the ternary polymers, which led to the shift of the carbonyl stretching absorption band of PVP. On the other hand, the melting, crystallization temperature, and crystallinity of the blends had a little change compared with the neat PVDF in the first heating process. Except for the content of PVP containing 30 wt %, the crystallinity of PVDF decreased remarkably from 64% to 33% and the value of $t_{1/2}$ was not obtained. Besides, the hydrophilicity of PVDF was remarkably improved by blending with PMMA/PVP, especially when the content of PVP reached 30 wt %, the water contact angle displayed the lowest value which decreased from 98.8° to 51.0°. © 2012 Wiley Periodicals, Inc. J. Appl. Polym. Sci. 000: 000–000, 2012

KEYWORDS: poly(vinylidene fluoride) (PVDF); poly(methyl methacrylate) (PMMA); poly(vinyl pyrrolidone) (PVP); crystallization; hydrophilicity

Received 10 September 2011; accepted 18 March 2012; published online 00 Month 2012
DOI: 10.1002/app.37718

INTRODUCTION

Poly(vinylidene fluoride) (PVDF) is a semicrystalline thermoplastic polymer with five distinct crystal polymorphs depending on the crystallization conditions, including α, β, γ, δ, and ε phases. The different crystal phases are associated with the varying properties of polymer. The first two are the main crystalline phases. The non-polar α phase is the most common form with the *trans-gauche-trans-gauche′* (TGTG′) conformation,[1] as well as excellent mechanical properties. These properties make α phase PVDF a good electro-optical storage material, which can be used for specific optical, chemical, electronic, and solar energy devices. The polar β phase, which is responsible for the piezo and pyro-electrical properties, presents all *trans*-TTT planar zigzag structure.[2] In recent years, study on how to control and improve the content of α phase or β phase has been developed widely.

On the other hand, PVDF is a well known polymer for thermal, chemical, oxidation resistance, and exceptional hydrolytic stability. The crystalline phase of the polymer provides thermal stability while the amorphous phase accommodates the desired membrane flexibility. All these properties make PVDF as an attractive material for various separation processes. However, the high crystallinity and low surface tension properties give it very low permeation values. During the ultrafiltration process, high hydrophobic property and low fouling resistance PVDF membrane is susceptible to the fouling of proteins, which limits

its application. Polymer blending has been known to be the most frequently used means of overcoming the shortcomings of an individual polymer and of obtaining inexpensive materials with desirable properties by combining the advantages of two or more individual polymer components. Therefore, an efficient method to improve the hydrophilicity of PVDF is polymer blending with hydrophilic polymers. In recent years, PVDF is often blended with oxygen containing polymers, such as poly (vinyl acetate) (PVAc),[3] poly(ethylene glycol) (PEG),[4] poly (methyl methacrylate) (PMMA),[5–7] and poly(vinyl pyrrolidone) (PVP).[8] As PVDF is highly miscible with oxygen containing polymers, which is related to the interaction between the fluorine atoms and carbonyl groups of the partner polymer. Among these polymers, PMMA has been the most studied compatible polymer with PVDF owing to cost, optical properties, solvent resistance, and performance advantages. Previous reports[5–7] have demonstrated that PVDF and PMMA are molecularly miscible in the amorphous state, and the blends have been studied extensively by thermal and morphology analyses. The properties of the blends are highly dependent on PMMA content. The PVDF/PMMA blend with the mass ratio of 70/30 exhibits the best balance of hydrophilicity, optical properties, hardness, mechanical strength, and weatherability.[5] PVDF/PVP is also a miscible blend, and the hydrophilicity of PVDF is remarkable improved by blending PVP, which is due to PVP existence of excellent hydrophilicity.[8] Moreover, the PMMA chains are susceptible to entangle with PVP chains by the dipole–dipole interactions, as well as PMMA segment having the good compatibility with PVP.[9] Considering that the effects of crystallization behavior and hydrophilicity in the PVDF/PMMA/PVP ternary blends have been less investigated, a series of PVDF/PMMA/PVP blends were prepared by solution casting in this work. The crystallization behavior of blends was investigated by Fourier transform infrared spectroscopy (FTIR), wide angle X-ray diffraction (WAXD), and differential scanning calorimetry (DSC). Simultaneously, the morphology and hydrophilicity of blends were also measured by scanning electron microscope (SEM) and contact angle test.

EXPERIMENTAL

Materials

PVDF (Kynar K 760, $\overline{M_w}$= 371,000) was supplied by Elf Atochem of North America. PMMA resin (HR1000L $\overline{M_w}$ = 110, 000) was obtained from Kurkaray (Japan). PVP (K30 $\overline{M_w}$ = 40,000) was purchased from Xilong Chemical Reagent (China). *N,N*-dimethylformamide (DMF, purity, ≥99.5%) was supplied from Sinopharm Chemical Reagent (China). All the chemicals were used as received.

Sample Preparation

The blends of PVDF/PMMA/PVP with different mass ratios were dissolved in DMF at 40°C with continuous stirring for 5 h. The initial polymer concentration of the solution was 5 wt %. Then, the resulting solution was spread on a glass substrate and kept at 40°C in a vacuum oven for 72 h. Finally, the blend film was cooled at room temperature, and peeled from the glass substrate. A set of the blend films with various mass ratios of PVDF/PMMA/PVP containing 70/30/0, 70/20/10, 70/15/15, 70/10/20, and 70/0/30 (w/w/w) were obtained.

Characterization Techniques

Scanning Electron Microscope. Scanning electron microscopy micrographs of the surfaces and cross-sections of various blends were obtained by a JSM-5900LV (JEOL, Japan) instrument with an accelerating voltage of 15 kV. The cross-sections were obtained by frozen-fracture of sample films immersed in liquid nitrogen and coated with gold.

Fourier Transform Infrared Spectroscopy. FTIR spectroscopy spectra were recorded with an IFS 66/S (Bruker, Germany) using the dry blend films. Each spectrum was obtained by performing 32 scans between 4000 and 400 cm^{-1} with a resolution of 4 cm^{-1}.

Wide Angle X-Ray Diffraction Measurement. WAXD diffractograms were obtained by an XRD-6000 diffractometer (Shimadzu, Japan) to analyze the crystalline phase of samples at room temperature. The radiation source (Cu K_α X-ray) was operated at 40 kV and 30 mA, with the scanning angle ranging from 5° to 50° and the scanning velocity of 4°/min.

Differential Scanning Calorimetry. DSC was performed on a Q-200 thermal analysis apparatus (TA Instruments, USA). The polymer samples (ca. 10 mg) were heated from room temperature to 200°C at the rate of 10 °C/min and kept at 200°C for 3 min. And then the samples were cooled to 40°C at a rate of 5 °C/min and maintained at 40°C for 1 min to obtain the crystallization curves. In order to observe melting processes of the samples which erased the thermal history, the second heat running was made from 40°C to 200°C at 10 °C/min. All the samples were measured at least three times to get errors of DSC data. The crystallinity (X_c) of PVDF was calculated by[10]

$$X_c = \frac{\Delta H_f/\phi}{\Delta H_f^*} \times 100\% \quad (1)$$

where $\Delta H_f^* = 104.5$ J/g is the melting enthalpy for a 100% crystalline PVDF, ΔH_f is the melting enthalpy of the blends measured in DSC, and ϕ is the weight fraction of PVDF in PVDF/PMMA/PVP blends. The crystallization half time ($t_{1/2}$), which is defined as the half time of crystallization, was used as a characteristic parameter of the crystallization process.[11]

Contact Angle Measurements. Static contact angles of the samples surface were measured using the sessile drop method with a DSA-100 goniometer (Krüss, Germany) at 23°C. Deionized water and diiodomethane were applied as the test liquids. The image of liquid drop (volume of 2 μL) was recorded by a video camera and fitted by mathematical functions. To establish the balance of the forces involved, the contact angle reading was obtained after 20 s deposition of the drop on the surface of the samples. Each contact angle was an average of at least five measurements, with the accuracy of ±2°. Finally, the total solid surface tension γ_s, and its dispersive γ_s^d and polar component γ_s^p were calculated by the Owens and Wendt method.[12]

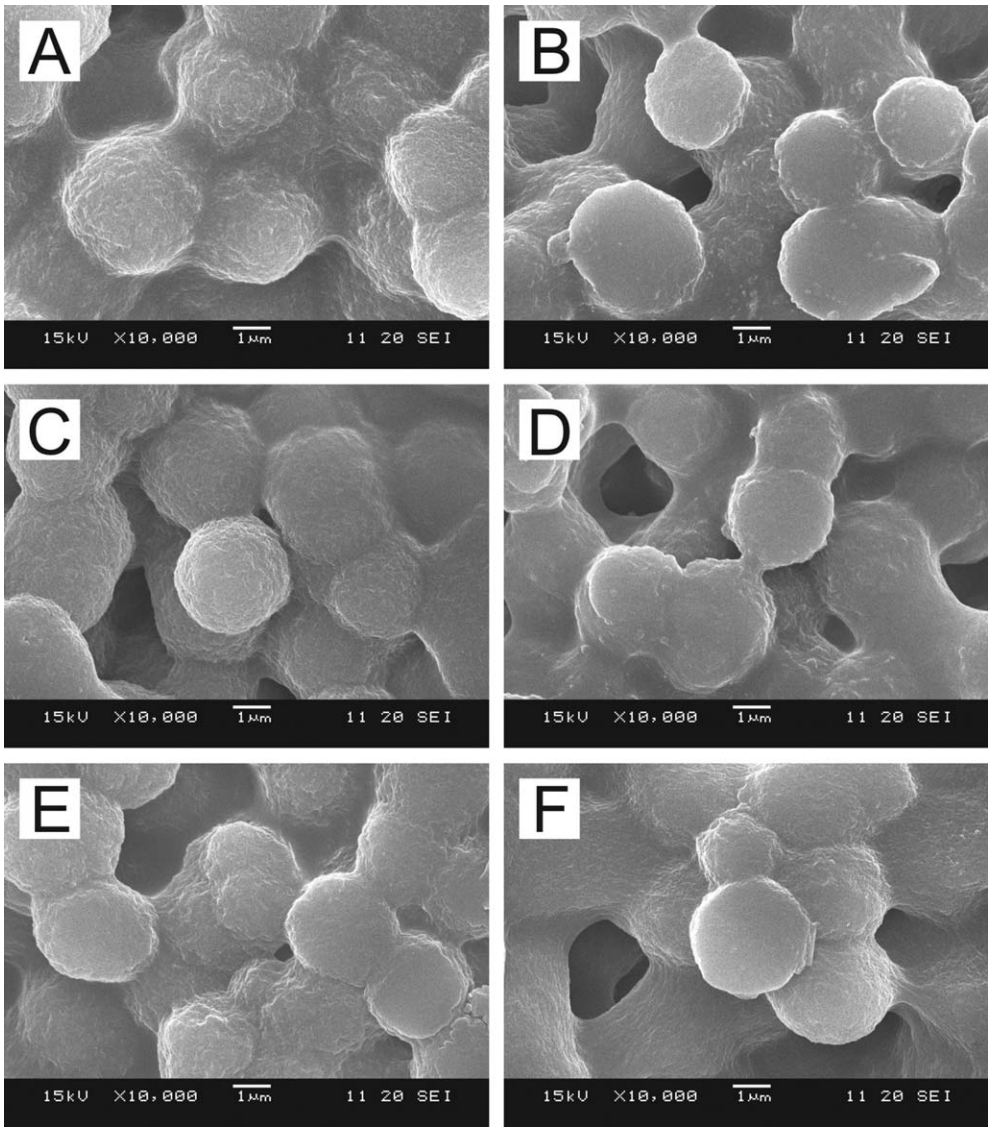

Figure 1. SEM micrograph top surface of PVDF/PMMA/PVP blends with various mass ratios: (A) 70/30/0; (B) 70/20/10; (C) 70/15/15; (D) 70/10/20; (E) 70/0/30; (F) neat PVDF.

RESULTS AND DISCUSSION

SEM Morphology

The morphology of the various samples generated at the air/solution interface is shown in Figure 1. It can be clearly observed that the surface was full of typical spherulitic structure of PVDF and the average diameter was in the order of 3 μm. Moreover, the size of surface spherulites had little change with the PMMA or PVP addition. It indicated that the introduction of PMMA/PVP blend into PVDF did not affect the growth of the surface spherulites via solution casting. This phenomenon may be explained by crystallization mechanism at the air/solution interface and surface enrichment of PVDF. The size of the spherulites depended on the temperature of crystallization and on the space of the nuclei from which they grew.[13–15] The PVDF chains expanded effectively in good solvent (DMF) and were susceptible to arrange into the crystal lattice. During the evaporation, the solvent in the air/solution interface must evaporate quickly and the interface first reached the crystallization concentration (the critical concentration before crystallization). A concentration difference will exist between the interface and the bulk solution. The larger the concentration difference, the higher the driving force for the mobility of the polymer chains in the solution. Thus, the preferential formation of nuclei on the top surface (at the air/solution interface) occurred due to the presence of the degree of super saturation for PVDF crystallization. On the other hand, the lower surface free energy component of polymer blend is enriched at the surface in order to minimize the interfacial free energy.[8,16,17] A previous investigation of PVDF blended with various amorphous polymers had shown that the concentration of PVDF present at the air/surface was greater than that in the bulk. Such surface enrichment has also been observed for fluorochemical-doped polymers and for other polymer blends.[8,17]

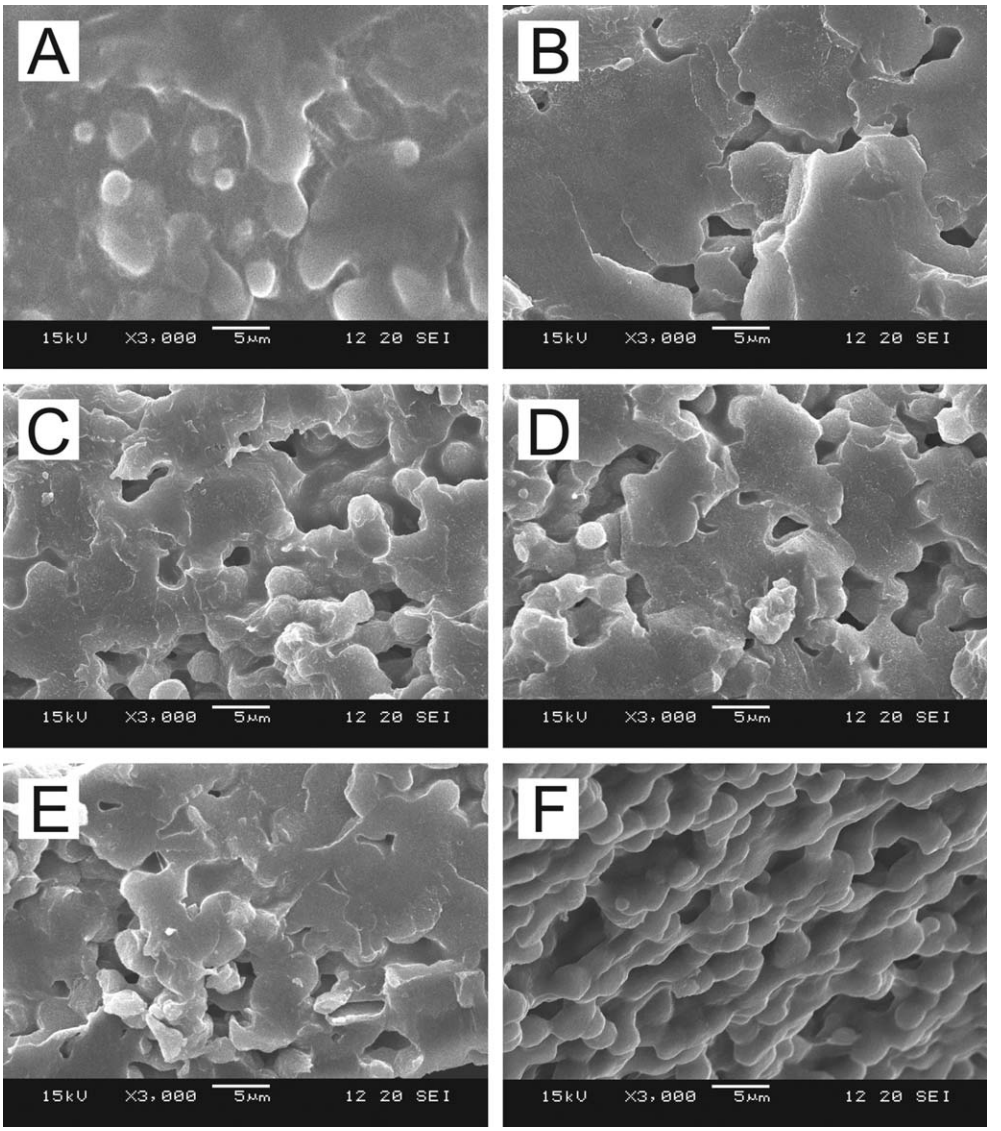

Figure 2. SEM micrograph of cross-section of PVDF/PMMA/PVP blends with various mass ratios: (A) 70/30/0; (B) 70/20/10; (C) 70/15/15; (D) 70/10/20; (E) 70/0/30; (F) neat PVDF.

The SEM observation of the cross-section is a qualitative way to confirm the phase morphology of this polyblend. Figure 2 shows the microscopic investigation of the cross-section of the ternary blends with various mass ratios of each component. As shown in Figure 2, the cross-section of neat PVDF exhibited full of typical spherulites with average diameter of 3 μm. Compared with the fracture surface of neat PVDF, a small amount of spherulites was also observed in the ternary blends. Meanwhile, there was no distinguishable boundary at the polymer interfaces and cross-section of each sample seemed to be almost a single phase system. It revealed that all PVDF/PMMA/PVP blends with various mass ratios, to a great extent, were compatible. In the literatures, PVDF is miscible with a number of carbonyl-containing polymers, which is attributed to polar interactions between CF_2 and C=O groups.[6,8,18] Additionally, Chen et al.[9] reported that PVP/PMMA blends were all miscible because of the dipole–dipole interactions.

FTIR Spectroscopy

FTIR is an effective way to characterize different groups and their interactions in the blends, and it can also distinguish the different crystalline phases of PVDF. In this work, the FTIR spectra of the neat PVDF, PMMA, PVP, and ternary blends (PVDF/PMMA/PVP) with various mass ratios are shown in Figure 3. It can be clearly observed that the absorption peaks of samples [Figure 3(A–F)] presented at 510 cm^{-1} (CF_2 bending) and 839 cm^{-1} (CH_2 rocking), which was assigned to the β phase crystal of PVDF.[19] It indicated that β phase of PVDF predominates in the crystallization by solution casting. The presence of the absorption band at 1729 cm^{-1}, attributable to the stretching of the carbonyl group, was used to characterize the existence of PMMA in the blend. The bands at 1149, 1192, 1241, and 1270 cm^{-1} represented C—O—C stretching vibration in PMMA.[20] However, with the decrease of PMMA content, the intensity of characteristic band of PMMA became weaker and

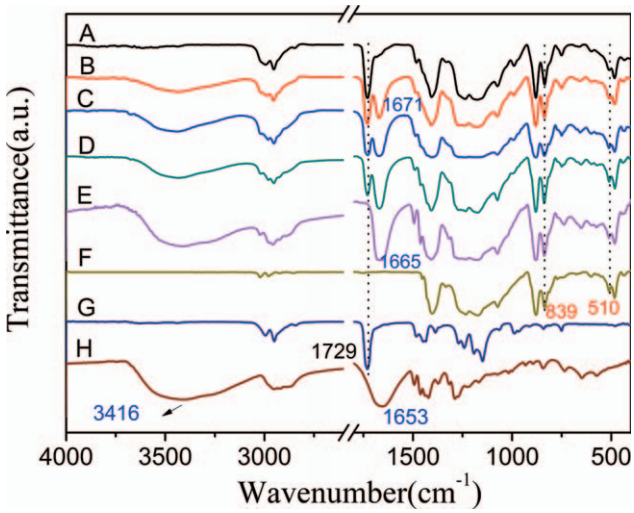

Figure 3. FTIR spectra of PVDF/PMMA/PVP blends with various mass ratios: (A) 70/30/0; (B) 70/20/10; (C) 70/15/15; (D) 70/10/20; (E) 70/0/30; (F) neat PVDF; (G) neat PMMA; (H) neat PVP. [Color figure can be viewed in the online issue, which is available at wileyonlinelibrary.com.]

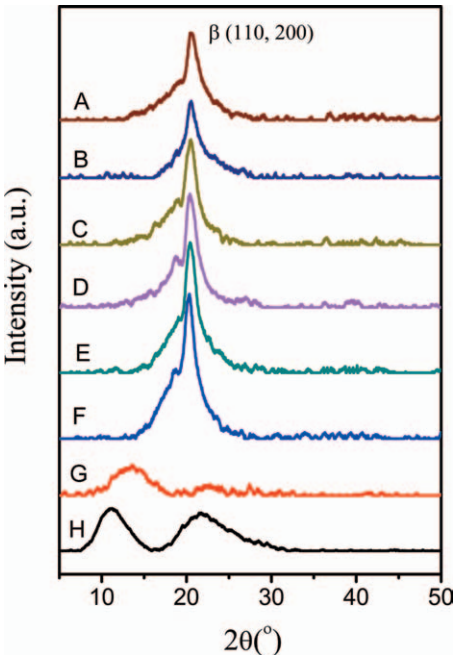

Figure 4. X-ray diffractograms of PVDF/PMMA/PVP blends with various mass ratios: (A) 70/30/0; (B) 70/20/10; (C) 70/15/15; (D) 70/10/20; (E) 70/0/30; (F) neat PVDF; (G) neat PMMA; (H) neat PVP. [Color figure can be viewed in the online issue, which is available at wileyonlinelibrary.com.]

eventually disappeared when the content of PVP reached 30 wt %. In the inset of Figure 3(H), the main feature of the IR spectrum of PVP, which contained an amide carbonyl, was a strong band at 1653 cm^{-1}. Other bands were centered at 1462 cm^{-1} and 1422 cm^{-1} which resulted from the vibration of the tertiary nitrogen, and a broad absorption band at 3416 cm^{-1} corresponds to OH stretching vibration.[21] In the spectra, the carbonyl stretching absorption band of PVP located at 1653 cm^{-1} shifted to higher frequencies by up to 12 cm^{-1} with containing 30 wt % PVP in the blend. This observation can be explained by the effect of forming specific hydrogen bonding between C=O of PVP and CH_2 of PVDF; the hydrogen bonding restricted the vibration of C=O bond and hence increased the absorption frequency.[8] However, with the addition of PMMA in the blend, the shift of the carbonyl stretching absorption band of PVP increased by 18 cm^{-1}, which was higher than the shift in the PVDF/PVP binary blend. It was attributed to the dipole–dipole interaction between PMMA and PVP chains. This was in agreement with results reported by Chen et al.[9]

WAXD Analysis

In order to further check the predominating crystalline phase, XRD of the ternary blends and neat polymers were obtained, as shown in Figure 4. Neat PMMA and PVP exhibited an amorphous feature that was characterized by the amorphous halos with no sharp peaks [Figure 4(G,H)]. By contrast, other samples displayed a sharp diffraction peak at $2\theta = 20.6°$, which was attributed to β phase, corresponding to the reflections of the (110) and (200) crystal planes.[5] This was totally in agreement with the results of FTIR, in which absorption bands at 840, 510 cm^{-1} were the characteristic bands of β phase. The polar solvent DMF played an important role in the formation of this phase. As reported, the dipolar interactions and hydrogen bonding between crystal nucleus of PVDF and DMF molecular chains promoted the *trans*-planar of CH_2—CF_2, which was favorable to form the β phase crystal of PVDF.[22] On the other hand, several papers have reported that PVDF blended with polar polymer favored to develop the β phase crystal of PVDF due to the strong dipolar/hydrogen bonding interactions between the counterpart polymer and PVDF.[23]

Thermal Analysis

Figure 5(a) showed the first heating curves of PVDF and blend samples from solution casting and the detailed melting data are given in Table I. As shown in Table I, the melting peak temperature (T_m^p) of neat PVDF was 171.5°C. The melting peak

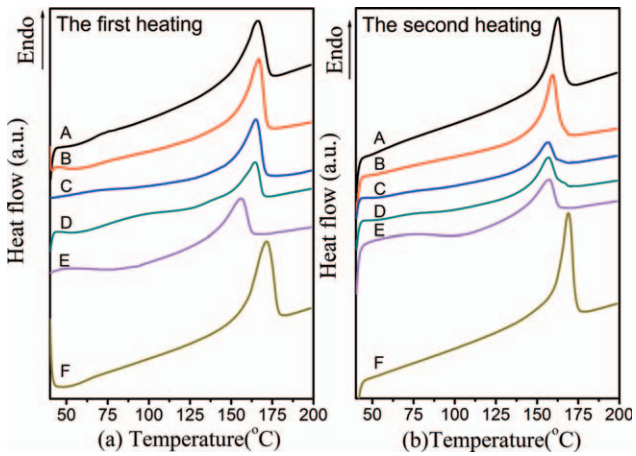

Figure 5. The first and second heating curves of PVDF/PMMA/PVP blends with various mass ratios: (A) 70/30/0; (B) 70/20/10; (C) 70/15/15; (D) 70/10/20; (E) 70/0/30; (F) neat PVDF. [Color figure can be viewed in the online issue, which is available at wileyonlinelibrary.com.]

Table I. DSC Parameters from First Heating Scan and Cooling Crystallization of Ternary Blends Containing PVDF

Samples	T_m^{on} (°C)	T_m^p (°C)	T_m^f (°C)	ΔT_m (°C)	ΔH_m (J/g)	X_c (%)	T_c^p (°C)	ΔH_c (J/g)	$t_{1/2}$ (min)
PVDF/PMMA/PVP blends (wt %)									
70/30/0	149.5 ± 1.0	165.8 ± 0.1	173.2 ± 0.1	23.7	45.9 ± 2.0	62.8 ± 2.3	126.8 ± 0.7	29.8 ± 2.1	2.01 ± 1.4
70/20/10	151.9 ± 0.2	166.6 ± 0.1	171.4 ± 0.3	19.5	49.0 ± 0.7	66.9 ± 0.9	118.4 ± 0.4	28.3 ± 1.7	1.86 ± 0.9
70/15/15	147.3 ± 0.2	163.4 ± 0.6	169.1 ± 0.1	21.8	46.5 ± 1.7	63.6 ± 2.0	119.1 ± 0.2	30.2 ± 0.6	2.06 ± 0.5
70/10/20	152.3 ± 0.3	166.5 ± 0.1	171.1 ± 0.7	18.8	41.2 ± 0.1	56.3 ± 0.2	120.1 ± 0.7	30.5 ± 3.0	2.35 ± 0.8
70/0/30	140.6 ± 0.4	155.7 ± 0.3	161.2 ± 0.2	20.6	24.5 ± 2.4	33.5 ± 3.2	-	-	-
PVDF	156.9 ± 0.1	171.5 ± 0.7	177.8 ± 0.7	20.9	67.5 ± 0.7	64.6 ± 0.3	143.6 ± 0.5	43.5 ± 2.0	0.91 ± 0.3

T_m^{on}: onset melting temperature; T_m^p: peak melting temperature; T_m^f: final melting temperature; $\Delta T_m = T_m^f - T_m^{on}$; ΔH_m: melting enthalpy; X_c: crystallinity of PVDF; T_c^p: peak crystallization temperature of PVDF; ΔH_c: crystallization enthalpy of PVDF.

temperature slightly decreased with the addition of PMMA/PVP blend. Moreover, the crystallinity (X_c) of PVDF had a little change in the ternary blends, except that only PVP was blended with PVDF. This could be explained by the effect of solvent evaporation on crystallization. The crystallization rate is intimately related to the evaporation rate of the solvent.[22] The blend films crystallized from DMF solution at same concentration (5 wt %), similar to evaporation rate of solvent under the same working conditions, which led to similar crystallinity when the effect of solvent evaporation on PVDF crystallization was dominant. Moreover, in a good solvent (DMF), PVDF chains can be completely dissolved and expanded, leading to more flexible, when crystallization occurred, these chains were easy to arrange into the lattice resulting in the high crystallinity (i.e., the crystalllinity of PVDF reached more than 60%). Nevertheless, with respect to PVDF/PVP binary blend, a strong hydrogen-bonding contributed to interaction between C=O of PVP and CH_2 of PVDF.[8] The effect of interaction between PVP and PVDF possibly became preponderant relative to effect of solvent evaporation. Consequently, the PVP chains entangled closely with the PVDF chains, which obviously hindered the macromolecular folding, resulting in the crystallinity of PVDF decreasing greatly.

After heating to above the melting temperature and then cooling, the samples remove the thermal history by the second heating, as shown in Figure 5(b). It was obviously observed that the values of T_m^p in the second temperature rising were lower compared with the data from the first temperature rising. As reported,[24] the melting peaks of α- and β-PVDF were so close that the difference between them was only 3°C (the α-PVDF has the lower melting peak temperature). As demonstrated in our previous work,[24] the ternary blends presented predominantly β phase of PVDF by solution casting. Therefore, in the first melting curve, the melting peak at the higher temperature was in correspondence with the β phase. On the other hand, the crystallization of PVDF was from the melt and the second heating run presented predominantly melting of α phase. This can be explained that the T_m^p of the second temperature rising were lower compared with the data from the first temperature rising. As shown in Table II, increasing the content of PVP, the values of ΔH_m (enthalpy of melting) and X_c had a downward trend. Furthermore, they were markedly lower than the results of the first heat running. This can be explained by the different crystallization mechanism of PVDF, i.e., prepared from solution casting and melting process.

Figure 6 displays the DSC crystallization thermograms of blends with different compositions containing neat polymer during cooling from the melt at 5 °C/min. The crystallization data are listed in Table I. Obviously, a sharp exothermic peak was observed at about 143.6°C because of the crystallization of neat PVDF. When 30 wt % PMMA was blended with PVDF, the crystallization peak temperature (T_c^p) significantly decreased. Additionally, with the addition of PVP, the endothermic traces for the melt-crystallization process became wider and shifted towards lower temperatures, eventually disappeared when the content of PVP was 30 wt %. On the other hand, the crystallization half time ($t_{1/2}$), which is defined as the half time of crystallization, was used as a characteristic parameter of the crystallization process. As reported, the smaller the value of $t_{1/2}$ was, the faster the crystallization rate was, and vice versa.[25] In Table I, it was obviously observed that the values of $t_{1/2}$ of the ternary blends were higher than that of neat PVDF. This

Table II. DSC Parameters from Second Heating Scan of Ternary Blends Containing PVDF

Samples	T_m^{on} (°C)	T_m^p (°C)	T_m^f (°C)	ΔT_m (°C)	ΔH_m (J/g)	X_c (%)
PVDF/PMMA/PVP blends (wt %)						
70/30/0	153.4 ± 0	162.5 ± 0.2	166.8 ± 0.3	13.5	37.7 ± 2.5	51.6 ± 2.4
70/20/10	149.0 ± 0.2	159.3 ± 0.1	164.9 ± 0.2	15.9	35.9 ± 0.1	49.0 ± 0.2
70/15/15	143.4 ± 1.1	156.3 ± 0.6	161.8 ± 0.4	18.4	31.2 ± 2.9	42.6 ± 3.1
70/10/20	144.1 ± 0.5	157.3 ± 1.0	164.7 ± 1.3	20.5	26.1 ± 0.1	35.7 ± 0.2
70/0/30	140.9 ± 0.3	157.5 ± 0.4	166.2 ± 2.5	25.3	22.0 ± 3.1	30.1 ± 4.2
PVDF	159.8 ± 0	168.6 ± 0.9	174.3 ± 1.4	14.5	55.5 ± 2.5	53.1 ± 2.3

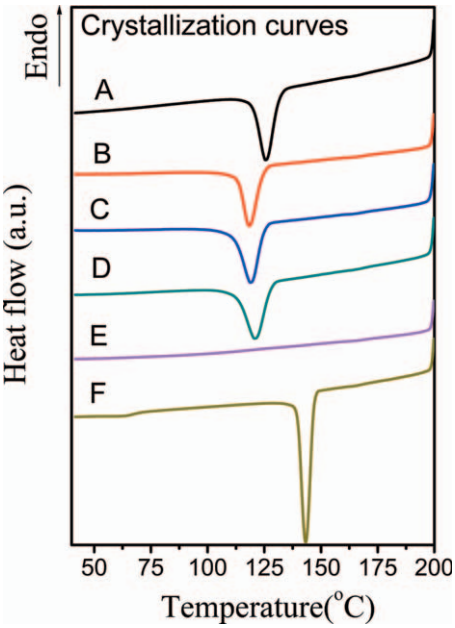

Figure 6. DSC crystallization curves of PVDF/PMMA/PVP blends with various mass ratios: (A) 70/30/0; (B) 70/20/10; (C) 70/15/15; (D) 70/10/20; (E) 70/0/30; (F) neat PVDF. [Color figure can be viewed in the online issue, which is available at wileyonlinelibrary.com.]

probably occurred because PMMA/PVP blends acted as diluents and reduced the crystallization rate of PVDF.[22] It was noteworthy that the endothermic trace and value of $t_{1/2}$ were not obtained as the content of PVP reached 30 wt %. This could be explained that a strong hydrogen bond interaction between PVP and PVDF interrupted the chains of PVDF to fold and stack, resulting in slower crystallization rate, even giving rise to sample without crystallization.[26] What's more, it is worthwhile to note that 30 wt % PVP in the blends [trace E in Figure 5(b)] exhibited a wide exothermic peak, which was attributed to cold crystallization process of PVDF. It was demonstrated that there was a stronger interaction of PVDF with PVP rather than with

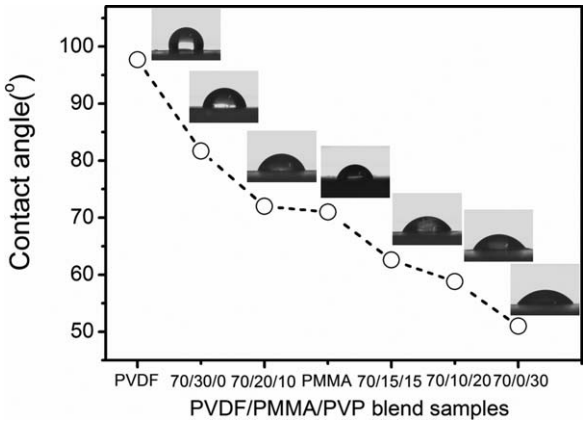

Figure 7. Contact angles of PVDF/PMMA/PVP blends with various mass ratios.

PMMA. This observation was in agreement with FTIR results discussed in the previous section.

Contact Angle Measurements

Contact angle measurements are widely used as a simple, sensitive technique for quantifying the hydrophilic/hydrophobic property of a surface. In general, the lower the contact angle against water, the more hydrophilic the sample is. The values of the contact angles PVDF/PMMA/PVP blends and neat PVDF are illustrated in Figure 7. The contact angle of the neat PVDF was 98.8°, which was a typical contact angle of hydrophobic surface. When PMMA content increased to 30 wt %, the water contact angle reduced to 81.7°. What's more, with the content of PVP adding in the ternary blends, the contact angle of blend surface dramatically decreased. Especially, when the content of PVP reached 30 wt %, the water contact angle displayed the lowest value which decreased to 51.0°. It indicted that introduction of PVP could significantly improve the hydrophilicity of PVDF.

Contact angle measurements of a 2 μL water droplet on the blend films are displayed in Figure 8. PVP is a water soluble polymer. When the water drop contacted PVP film surface, the

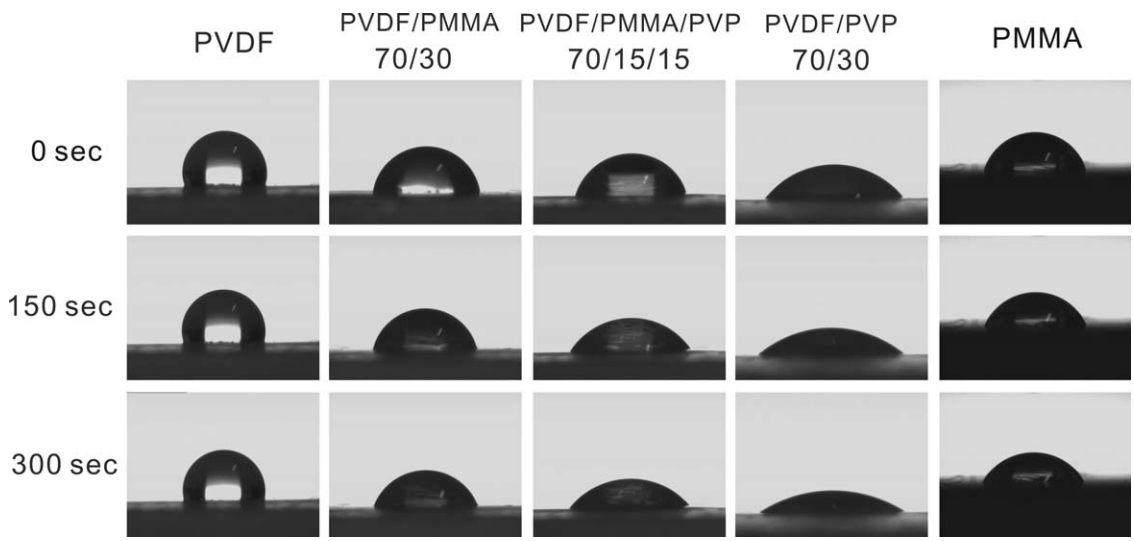

Figure 8. Changes in contact angle with water drop time.

Table III. Contact Angles of Distilled Water and Diiodomethane, and Solid Surface Tensions γ_s and Components γ_s^d and γ_s^p

	Contact angle (°)		Surface tensions (mJ/m^2)		
Surface	Distilled water	Diiodomethane	γ_s	γ_s^d	γ_s^p
PVDF/PMMA/PVP blends (wt %)					
70/30/0	81.7	44.5	38.84	33.94	4.89
70/20/10	72.0	41.6	43.00	33.85	9.15
70/15/15	62.6	53.8	43.43	25.60	17.83
70/10/20	58.8	46.2	47.78	29.26	18.52
70/0/30	51.0	39.4	54.01	31.76	22.26
PVDF	98.8	59.5	28.94	27.57	1.37

γ_s: solid surface tension; γ_s^d: dispersive solid surface tension; γ_s^p: polar solid surface tension.

complete wetting occurred. This contact angle cannot be measured. Thus, we did not display the digital photo of PVP film in Figures 7 and 8. The PVDF/PVP binary blend surface exhibited instantaneous wetting as the water droplet spontaneously spread onto the surface. A remarkable decrease in contact angle occurred, which reduced from 52.3° to 31.0° after 5 min, indicating water absorption into PVP macromolecules. By contrast, a PVDF control film (Figure 8, left) displayed hydrophobic behavior with a contact angle of 104°. With the water drop time increasing, the contact angle slightly decreased by only 6° due to the evaporation of water drop. The contact angle of PMMA film (Figure 8, right) decreased from 72.0° to 58.1°. With respect to the PVDF/PMMA binary blend, the water contact angle was 83.6° in the instantaneous, which was attributed to the hydrophilicity of PMMA chains. Meanwhile, a continuous decrease in contact angle from 83.6° to 71.8° exhibited the change of PVDF surface from hydrophobic into hydrophilic surface. Similarly, as the PVP content reached 15 wt %, the contact angle of ternary blend reduced from 71.5° to 50.0° after 5 min.

By measuring the contact angle for two different test liquids, the surface tension γ_s, which consists of the two components of dispersive part γ_s^d and polar part γ_s^p is obtained. The detailed results are given in Table III. The neat PVDF exhibited a low surface tension (γ_s = 28.94 mJ/m^2), whose polar part γ_s^p was only 1.37 mJ/m^2. However, when PMMA content reached 30 wt %, the polar component increased to 4.89 mJ/m^2. Meanwhile, with the content of PVP adding, the polar part of ternary blend surface increased markedly from 4.89 to 22.26 mJ/m^2, which was 16 times of the value of neat PVDF. Additionally, the polar component exhibited the highest when only PVP was blended with PVDF. This agreed with the result of water contact angle. It implied that the polar component played an important role in the hydrophilicity of the blends. Moreover, the increase in surface tension was mainly due to incorporation of polar groups on to the ternary blend surfaces (Table III). According to the literatures, the hydrophilicity of PMMA is related to the contributions of the dipole–dipole and dipole-induced-dipole interaction,[6] while the hydrophilicity of PVP is attributed to strong polarity and hydrophilic groups.[27,28] In this case, the high compatibility of PVDF/PMMA/PVP ternary blend was induced by strong interaction between the carbonyl groups of PMMA/PVP blend and CF_2 or CH_2 group of PVDF, which led to the significant improvement in the hydrophilicity of PVDF.

CONCLUSIONS

In this work, SEM, FTIR, WAXD, DSC, and contact angle measurements have been employed to investigate in detail the morphology, crystallization behavior, and hydrophilicity of PVDF/PMMA/PVP ternary blends. According to morphological analysis, the surface was full of typical spherulitic structure of PVDF and the average diameter was in the order of 3 μm. The samples presented predominantly β phase of PVDF by solution casting. It indicated that the size of surface spherulites and crystalline phase had little change with the PMMA or PVP addition. On the other hand, FTIR spectra demonstrated special interactions among the ternary polymers, which led to the shift of the carbonyl stretching absorption band of PVP. The melting, crystallization temperature, and crystallinity of the blends had a little change compared with the neat PVDF in the first heating process. Except for the content of PVP containing 30 wt %, the crystallinity of PVDF decreased remarkably from 64% to 33%. This result was attributed to the strong hydrogen-bonding interaction between PVDF and PVP chains. The contact angle measurements and values of surface free energy showed that the hydrophilicity of PVDF was remarkably improved by blending with PMMA/PVP, especially when the content of PVP reached 30 wt %, the water contact angle displayed the lowest value which decreased from 98.8° to 51.0°. As a whole, it had been demonstrated that the PVDF/PMMA/PVP blend with mass ratio of 70/15/15 provided the best balance of the crystallinity and hydrophilicity.

ACKNOWLEDGMENTS

The financial support for this work was provided by the National Basic Research Program of China (2009CB623404) and the Priority Academic Program Development of Jiangsu Higher Education Institutions.

REFERENCES

1. Tripathy, S. K.; Potenzone, R.; Hopfinger, A. J.; Banik, N. C.; Taylor, P. L. *Macromolecules* **1979,** *12*, 656.
2. Pramoda, K. P.; Mohamed, A.; Yee Phang, I.; Liu, T. *Polym. Int.* **2005,** *54*, 226.
3. Chiu, H.-J. *J. Polym. Res.* **2002,** *9*, 169.
4. Zhao, Y. H.; Qian, Y. L.; Zhu, B. K.; Xu, Y. Y. *J. Membr. Sci.* **2008,** *310*, 567.
5. Ma, W.; Zhang, J.; Wang, X.; Wang, S. *Appl. Surf. Sci.* **2007,** *253*, 8377.
6. Huang, C.; Zhang, L. *J. Appl. Polym. Sci.* **2004,** *92*, 1.
7. Elashmawi, I. S.; Hakeem, N. A. *Polym. Eng. Sci.* **2008,** *48*, 895.
8. Chen, N.; Hong, L. *Polymer* **2002,** *43*, 1429.
9. Chen, W.-C.; Kuo, S.-W.; Jeng, U. S.; Chang, F.-C. *Macromolecules* **2008,** *41*, 1401.

10. Nakagawa, K.; Ishida, Y. *J. Polym. Sci. Polym. Phys. Ed.* **1973,** *11*, 2153.
11. Long, Y.; Shanks, R. A.; Stachurski, Z. H. *Prog. Polym. Sci.* **1995,** *20*, 651.
12. Owens, D. K.; Wendt, R. C. *J. Appl. Polym. Sci.* **1969,** *13*, 1741.
13. Zhao, X.; Cheng, J.; Chen, S.; Zhang, J.; Wang, X. *J. Polym. Sci. Part B: Polym. Phys.* **2010,** *48*, 575.
14. Ma, W.; Zhang, J.; Wang, X. *J. Macromol. Sci. B Phys.* **2008,** *47*, 139.
15. Ma, W.; Zhang, J.; Chen, S.; Wang, X. *J. Macromol. Sci. B Phys.* **2008,** *47*, 434.
16. Gu, X.; Michaels, C. A.; Nguyen, D.; Jean, Y. C.; Martin, J. W.; Nguyen, T. *Appl. Surf. Sci.* **2006,** *252*, 5168.
17. Tang, W.; Zhu, T.; Zhou, P.; Zhao, W.; Wang, Q.; Feng, G.; Yuan, H. *J. Mater. Sci.* **2011,** *46*, 1.
18. Landis, F. A.; Moore, R. B. *Macromolecules* **2000,** *33*, 6031.
19. Salimi, A.; Yousefi, A. A. *Polym. Test.* **2003,** *22*, 699.
20. Yan, H.; Zhang, X. H.; Wei, L. Q.; Liu, X. G.; Xu, B. S. *Powder Technol.* **2009,** *193*, 125.
21. Xu, M.; Shi, X.; Chen, H.; Xiao, T. *Appl. Surf. Sci.* **2010,** *256*, 3240.
22. Gregorio, R., Jr.; Borges, D. S. *Polymer* **2008,** *49*, 4009.
23. Zhong, G.; Zhang, L.; Su, R.; Wang, K.; Fong, H.; Zhu, L. *Polymer* **2011,** *52*, 2228.
24. Ma, W.; Zhang, J.; Wang, X. *J. Mater. Sci.* **2008,** *43*, 398.
25. Ma, W.; Zhang, J.; Chen, S.; Wang, X. *Colloid Polym. Sci.* **2008,** *286*, 1193.
26. Cheng, J.; Wang, S.; Chen, S.; Zhang, J.; Wang, X. *Polym. Int.* **2012,** *61*, 477.
27. Kireeva, P. E.; Shandryuk, G. A.; Kostina, J. V.; Bondarenko, G. N.; Singh, P.; Cleary, G. W.; Feldstein, M. M. *J. Appl. Polym. Sci.* **2007,** *105*, 3017.
28. Liu, X.; Fussell, G.; Marcolongo, M.; Lowman, A. M. *J. Appl. Polym. Sci.* **2009,** *112*, 541.